



S. Galeotti¹

DIEF—Department of Industrial Engineering of Florence, University of Florence, Via S. Marta 3, Firenze 50139, Italy
e-mail: sofia.galeotti@unifi.it

A. Picchi

DIEF—Department of Industrial Engineering of Florence, University of Florence, Via S. Marta 3, Firenze 50139, Italy
e-mail: alessio.picchi@unifi.it

R. Becchi

DIEF—Department of Industrial Engineering of Florence, University of Florence, Via S. Marta 3, Firenze 50139, Italy
e-mail: riccardo.becchi@unifi.it

R. Meloni

Baker Hughes, Via Felice Matteucci 2, Firenze 50127, Italy
e-mail: roberto.meloni@bakerhughes.com

G. Babazzi

Baker Hughes, Via Felice Matteucci 2, Firenze 50127, Italy
e-mail: giulia.babazzi@bakerhughes.com

A. Andreini

DIEF—Department of Industrial Engineering of Florence, University of Florence, Via S. Marta 3, Firenze 50139, Italy
e-mail: antonio.andreini@unifi.it

Impact of Fuel Injection System on the Performance of an Industrial Burner With Hydrogen Piloting Operated With Simulated Exhaust Gas Recirculation

Exhaust gas recirculation (EGR) can be exploited to increase the CO₂ content at the exhaust of gas turbines (GTs), in order to improve the efficiency of carbon capture systems. The lower oxygen level leads to challenging conditions for the combustion process, resulting in high CO and unburned hydrocarbon emissions and the possible onset of thermoacoustic instabilities. To mitigate these effects and expand the combustor's operational range, pilot flames can be employed to stabilize the combustion process, with localized hydrogen injections further enhancing reactivity. In this demanding and complex environment created by EGR, fuel injection strategy is crucial in the flame stabilization mechanism, and many design parameters come into play. The present work illustrates the results of an extensive screening performed in a single-cup atmospheric test rig at the THT Lab of the University of Florence, with EGR conditions simulated with CO₂ addition in the combustion air. In particular, six different configurations of a dry low NO_x industrial burner have been tested, varying the arrangement and geometry of the pilot jets, and the premix fuel injection mode. Burners' performance has been compared in terms of CO emissions, lean blow-out (LBO) limits, and dynamic behavior, and OH chemiluminescence imaging has also been employed to investigate the flame structure. The results point out that, for the investigated configuration, the occurrence of thermoacoustic instabilities is, together with CO emissions, the main limiting factor, but benefits have been observed with hydrogen addition, and promising configurations will be further tested in engine-like conditions.*

[DOI: 10.1115/1.4069776]

Introduction

Exhaust gas recirculation (EGR) is widely used in internal combustion engines as a strategy to reduce NO_x emissions [1]. The adoption in gas turbine (GT) systems on the other hand has been limited because of the high costs and complexity involved, which

are not easily justified when compared to the performance of existing emission control systems, such as dry low NO_x technologies. EGR becomes relevant in gas turbines frameworks when considered as a mean to enhance CO₂ concentrations in exhaust gases, for integration with carbon capture and storage (CCS) systems. Indeed, higher CO₂ concentrations increase the efficiency of carbon capture process [2], but typically low levels are encountered in GT exhaust because of lean conditions and secondary air dilution. The implementation of EGR allows to mitigate this limitation [3,4], improving the performance of the coupled GT-CCS system.

Turbo Expo: Turbomachinery Technical Conference & Exposition (GT2025), June 16–20, 2025, GT2025.

¹Corresponding author.

Manuscript received July 9, 2025; final manuscript received August 26, 2025; published online November 17, 2025. Editor: Jerzy T. Sawicki.

Early investigations into EGR's impact at engine conditions revealed positive effects for NO_x reduction [5–7], while lower oxygen levels in the recirculated oxidizer create challenging conditions for the combustion process, leading to increased emissions of CO and unburned hydrocarbons, which restrict the extent to which EGR can be applied [5,8–10]. Investigations with optical diagnostics revealed that CO_2 significantly affects flame structure and temperature [11] and CO_2 dilution reduces the smallest scales of flame wrinkling in turbulent methane–air flames, leading to lower turbulent burning velocities [12]. More recently, Rodriguez Camacho et al. [13] used CH^* chemiluminescence to show that diluents with different compositions have impacts on dynamic flame response, particularly at extremely low oxygen levels.

To address the challenges posed by these adverse effects, various solutions can be implemented to enhance the combustor operation under such demanding conditions. In the present study, an innovative approach introduced is the addition of a small amount of hydrogen with the pilot line. Studies by Oztarlik et al. [14] and Barbosa et al. [15] demonstrated that small hydrogen injections can stabilize thermoacoustically unstable flames and reduce oscillations, albeit with increased NO_x and, in some cases, CO emissions. Research by Shanbhogue et al. [16] further revealed how hydrogen blending alters flame dynamics by increasing the extinction strain rate, which impacts both flame holding and stability margins. Cheng et al. [17] confirmed that low-swirl injectors can handle significant hydrogen fractions without major system modifications, making hydrogen a viable solution for stabilizing flames in EGR conditions. Hydrogen applications within EGR systems can be found for internal combustion engines applications [18], while this approach remains largely unexplored for gas turbines. The most recent work of Rodriguez Camacho et al. [19] represents one of the first studies in this context focusing on the effect on the flame dynamic behavior.

This work is part of a wider research context, inside the European Project TRANSITION (fuTure hydRogen Assisted gas turbiNeS for effective carbon capTure IntegratiON) with the final goal of enhancing burner performance under challenging conditions involved by high EGR rates in gas turbines systems. In particular, an experimental campaign was conducted on an industrial burner in an atmospheric single-sector reactive test rig. This phase of the research can be considered the first stage of a design improvement to be placed inside a more general work frame, with test at atmospheric pressure allowing an extensive preliminary screening for exploring different solutions to improve flame stability. For replicating the lower oxygen level caused by EGR at lab scale, combustion air has been diluted with CO_2 , resulting in overall more challenging conditions for flame stability than real EGR because of the high CO_2 in the oxidizer [20]. This approach was chosen as it is convenient for storage purposes, while maintaining the main goal of comparing different solutions for enhancing burner performance under consistent conditions. The first stage of the investigation [21] presented a detailed characterization of the baseline burner configuration fueled only with natural gas (NG). In addition to studying behavior under conventional conditions, the effects of EGR were investigated, showing that as oxygen levels decrease, the flame becomes more widespread and shifts downstream. Higher CO emissions and thermoacoustic instabilities are recorded, limiting the performance under EGR conditions. The use of pilot hydrogen flames was explored in Ref. [20] to improve flame stability in order to limit the detrimental consequences of EGR. Hydrogen addition, whether blended with natural gas or injected as a pure stream, proved to be effective in mitigating these issues, reducing CO emissions, and improving the burner's dynamic behavior, both with and without EGR.

The present work represents a further step to enhance the performance of GT burners under the conditions generated by high EGR rates. In particular, various fuel injection solutions were tested for both the premix and pilot lines, as fuel distribution in the primary zone of the combustor plays a key role in stabilizing the flame. After a summary of the experimental setup employed for the investigation and the tested conditions, the performance of the new burner

configurations will be analyzed in terms of stability limits, emissions, and dynamic behavior, both with standard air as oxidizer and in EGR conditions. The effect of different fuel injection strategies on these parameters will be analyzed with the support of OH^* chemiluminescence imaging, which allows to see variations in the reaction zone structure, offering a detailed analysis of the effect of the different geometric feature. Finally, a summary of the performance of all the tested configurations will be presented.

Experimental Apparatus

Test Rig and Measurements. The experimental campaign took place at the THT Lab of the University of Florence, employing an optical reactive test rig with single-sector tubular chamber. A detailed description of the facility and the adopted test rig is available in Ref. [22]. Figure 1 reports a schematic of the facility, together with a picture of the reactive test rig. Briefly, dried compressed air is fed to the test rig by two screw compressors, with an electric heater preheating the airflow. CO_2 is injected in the combustion air upstream of the electric heater to lower the inlet oxygen content and reproduce EGR conditions. Downstream of the test section, a water jacket exhaust duct is installed, equipped with four water sprayers to quench the flue gases before the stack.

The test rig is fed by two natural gas lines, taken from the local gas network and compressed to 16 bars, while hydrogen is produced on demand with an electrolyzer, which can deliver up to 14,000 Nlt/h of hydrogen at 8 bar.

A cross section of the test rig is presented in Fig. 2(a), showing the tubular chamber enclosed in an outer vessel. The burner is installed on the upstream vessel, connected to the fuel lines with a dedicated flange. The outer downstream vessel is equipped with two perpendicular quartz windows to allow optical access on the flame. The combustion chamber consists of a 2.5 mm thick cylindrical quartz liner, held by rods and connected with a downstream metal duct which directs flue gases to the test rig's exhaust system. Liner's outer walls are cooled by forced convection, using a portion of incoming air that flows through the annular space between the liner and the confining vessel, bypassing the combustion process. The dome plate, different from the actual GT configuration, is equipped with effusion cooling holes, introducing cooling air into the combustion chamber to the burner main-flow. Ignition is achieved via a spark plug positioned along the flame tube downstream of the optical liner.

Regarding the measurement techniques, OH^* chemiluminescence imaging was employed to visualize the flame structure, implemented with a Phantom MIRO M340 camera coupled with the Hamamatsu C16031-311-Ax image intensifier. A bandpass filter ($\lambda = 310 \pm 5 \text{ nm}$) was mounted on a Nikon UV 105 mm $f/4.5$ lens to capture the OH^* transition, and images were acquired at 1000 Hz with 0.5 ms intensifier gate. Camera field of view (FoV) for OH^* chemiluminescence imaging is highlighted in Fig. 2(a), together with the coordinate system centered on the burner outlet.

CO and NO_x levels are measured with a HORIBA PG350 gas analyzer, after the exhaust is extracted from the flame tube about 350 mm from the burner exit, brought with heated pipeline kept at 150°C and dried before the analysis by a HORIBA PSS-5H refrigerator. Because of the wide variation in operating conditions in terms of fuel and oxidant composition, emission measurements are expressed as raw ppm measured by the gas analyzer on dry flue gas, with the same approach adopted in Ref. [8].

A high frequency pressure sensor (PCB) is used to detect the onset of thermoacoustic instabilities measuring pressure oscillations inside the combustion chamber ($f_{\text{aq}} = 12.8 \text{ kHz}$). It is installed downstream of the optical liner, at the same axial location as the emission probe. Pressure oscillations are characterized by their root mean square value, denoted as P'_{RMS} .

Investigated Burner Configurations. The burner concept investigated in this work is a well-established design employed by Baker Hughes for industrial gas turbine applications. Based on an

aeroderivative design, it offers versatility to operate stably under varying conditions [23], by minimizing the risks of flashback and auto-ignition while maintaining a compact combustor size. Turbulence is generated by two counter-rotating axial swirlers, with the burner architecture reported in the schematic of Fig. 2(b). Flowfield measurements performed in past test campaigns enlightened how this layout generates a jet-flame, without inner recirculation zone [20]. Indeed, the low swirl number of the counter-rotating swirler configuration is not sufficient to cause vortex breakdown to occur inside the combustion chamber, and only the external recirculation zone is present.

The burner features three independent fuel lines, in order to control pollutant emissions and at the same time ensure a stable combustion process also at partial load [24]. Premix line (PMX) injects the fuel at the tip of one of the two swirlers in a jet cross flow configuration. Strong mixing is ensured thanks to the intense turbulence created by the shear layer generated between the two swirlers in the converging nozzle, which accelerates the flow before entering the combustion chamber. Pilot line (PLT) injects the fuel directly into the combustor chamber through circumferentially equally spaced holes, giving rise to a diffusive flame front, helping the flame stabilization, and allowing safe and stable operation with different engine loads [25]. Center-body line (CB) injects the fuel along the burner axis in coflow with the incoming combustion air. Injection point is located upstream of the burner outlet, therefore ensuring a certain degree of premixing, although less than that achieved with the premix line. When it is not fed with fuel, the center-body is cooled by a small amount of purge air channeled through a hole along the burner axis. PMX and CB lines have been fed only with natural gas, while PLT holes can inject a fuel mixture going from pure natural gas to pure hydrogen. Fuel blending is realized upstream of the burner inlet, in correspondence with the flange connecting the burner to the test rig.

Different injection systems for both premix and pilot fuel have been tested, with a total of seven configurations, summarized in Table 1. The baseline configuration, which has been thoroughly characterized in previous works, is indicated as B0. In particular, the present study investigated the effect of different parameters:

- The pilot jet exit velocity was changed by varying the holes exit area (B1 and B4).
- Different jet orientations were tested varying the holes inclination ϕ (see Fig. 2(b)) (B1, B4, and B6).
- The number of pilot holes was varied from N to $2N$ to reduce jet penetration (B2).
- The premix fuel injection location was moved from the inner swirler (all new layouts).

Operating Conditions. Reactive tests have been performed at ambient pressure, and the lower oxygen level in the oxidizer caused by EGR has been reproduced by adding CO_2 to the combustion air. EGR condition is represented by the inlet oxygen mass fraction Y_{O_2} , which is a key similarity parameter between real EGR and simulated conditions. Even though CO_2 dilution is much more convenient than using nitrogen mixtures for the oxidizer to simulate EGR, tests with EGR-like conditions are still demanding in terms of gas consumption. Indeed, only a single EGR level has been tested, sufficiently high to push the burners to operate close to the stability limit, corresponding to $Y_{\text{O}_2} = 16.6\%$. This condition is referred to as “EGR” in the results discussion.

For each configuration, the total thermal power was computed to match the same adiabatic flame temperature in standard conditions with only natural gas, in order to have a fairly comparison. This was done to compensate small variations in the burner effective areas due to the 3D printing process, leading to slightly different oxidizer mass flow rate with the same pressure drop. Except for lean blow-out (LBO) tests, total thermal power (TP_{TOT}) has been kept constant for each configuration to such reference value (TP_{REF}), in order to

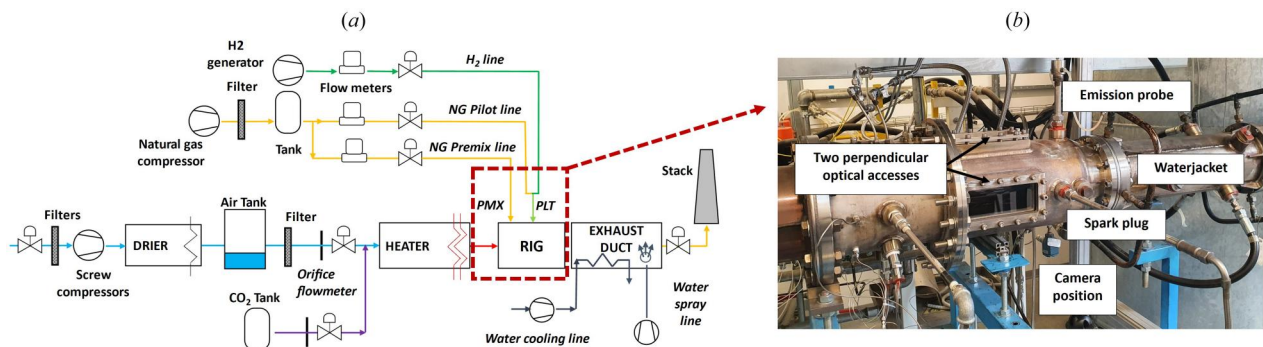


Fig. 1 Combustion test cell plant (a) and picture of the reactive test rig (b) at the THT Lab of the University of Florence

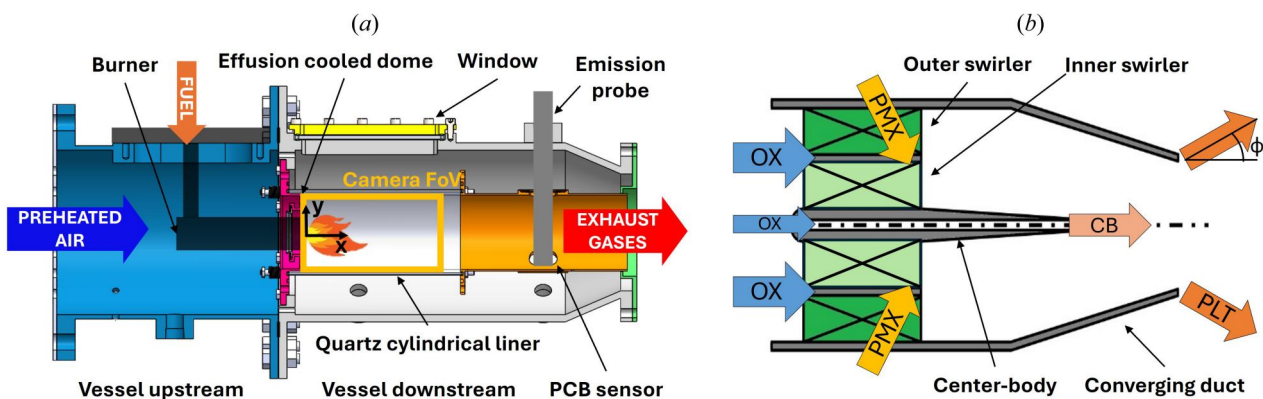


Fig. 2 Cross section of the reactive test rig (a) and investigated burner schematic (b)

Table 1 Investigated burner configurations

	PLT			PMX		CB
	N (-)	D (mm)	Direction	ϕ (deg)	Position	
B0	N	D	Outward	ϕ_{REF}	Inner swirler	—
B1	N	$1.2D$	Outward, swirled	ϕ_{REF}	Outer swirler	—
B2	$2N$	$0.7D$	Outward	ϕ_{REF}	Outer swirler	—
B4	N	$0.7D$	Straight	0	Outer swirler	—
B5-PMX	N	D	Outward	ϕ_{REF}	Outer swirler	—
B5-CB	N	D	Outward	ϕ_{REF}	—	YES
B6	N	D	$2 \times$ Outward	$2\phi_{REF}$	Outer swirler	—

compare different conditions because of the dual fuel configuration. For the same reason, fuel splits are defined with thermal power. PMX% is the thermal fraction of the premix line (always fully natural gas) over the total one. Split changes between the two fuel lines have been carried out to identify the most promising operational window for each configuration. TP(H₂) is the fraction of hydrogen thermal power over the total one, which includes both the premix and pilot contributions regardless of the fuel. The hydrogen fraction was maintained below 10% of the total thermal power, a value identified as an effective tradeoff. This limit ensures a balance between enhancing combustion stability and maximizing CO₂ content in the exhaust, aligning with the final goal of improving the efficiency of CCS integration [20].

The burner pressure drop has been kept at a reference value during the whole measurement campaign. Slight variations were measured for the test with simulated EGR, as the total mass flow rate of the oxidant was kept constant, while the composition of the mixture and thus the molecular weight varied. The inlet temperature of the oxidizer T_{inlet} was held constant at 300 °C. Summarizing, the investigated operating conditions are reported in Table 2.

Results and Discussion

The results start with the steady flame structure of the different burner configurations, since it helps to interpret and understand the following findings. Then, the burners' performance is presented, first under standard conditions without EGR, and second with simulated EGR, achieved by adding CO₂ to the combustion air. In particular, stability limits, pollutant emissions, and dynamic behavior will be presented, in order to investigate the effect of different fuel injection modes on the burner behavior. In the last part of the results, a summary of the main performance parameters is offered, with the purpose to highlight the major outcomes of this comparison.

Steady Flame Structure. The effect on the flame structure of different fuel injection modes has been investigated with OH* chemiluminescence. Time-averaged normalized OH* images are presented in Fig. 3 for different operating conditions: the first column reports the fully diffusive case with only natural gas, while the second and third columns refer to 50%PMX and [TP(H₂) = 5%] with standard air as oxidizer and in simulated EGR conditions, respectively.

Table 2 Tested operating conditions

T_{inlet}	300	(°C)
$\Delta P/P$	4.2	(%)
TP _{TOT}	TP _{REF}	(kW)
PMX%	0~95	(%)
TP(H ₂) %	0~5~10	(%)
Y_{O_2}	23.2~16.6	(%mass)

In the fully diffusive case (0%PMX), the reaction zone is lifted, with different extent for each configuration. In such conditions, some layouts give rise to a nonsymmetrical reaction zone (B1–B2 and B4), probably due to small geometrical differences in the holes exit, altering the jets velocity. At higher premix, the influence of the single pilot jets is reduced, and the flame returns approximately symmetrical. In all cases with higher premixing and doping the pilot jets with a small amount of hydrogen, the reaction zone comes closer to the burner exit and becomes more compact, both shorter and with reduced radial extension. The effect of simulated EGR (third column of Fig. 3) is consistent for all the tested configurations, with the reaction zone that shifts downstream and becomes widespread, as observed in previous works from the authors [20–22]. In this condition, the diffuse flame structure is similar among all the burner configurations, but some differences, especially at the flame base, can be enlightened. The extension of the region with high OH* values is similar, but the overall position varies. In particular, configuration B1 shows the flame located very close to the burner exit, while B5-PMX positions the flame further downstream compared to the other layouts. Additionally, in some cases (B0 and B4), a more pronounced curvature at the flame base is visible, anchoring near the pilot jets closer to the burner exit.

Results Without Exhaust Gas Recirculation (Standard Air as Oxidizer). A key factor in burner design is its ability to maintain stable combustion, which becomes even more critical in the perspective of operation with high EGR rates. With this purpose, LBO tests have been performed in order to explore the stability limits of the different burner configurations, for two fuel splits. In each case, starting from stable conditions, the fuel mass flow rate was gradually decreased while keeping constant the pressure drop across the combustion chamber and therefore the air mass flow rate, until the flame extinguished. The blow-out event was identified by looking at the pressure oscillations detected with the high frequency pressor sensor, which drop sharply when blow out is reached. The procedure was repeated three times for each case, showing great repeatability of the results.

Results are reported in terms of fraction of the reference thermal power at blow out in Fig. 4. Following the expected behavior with lower premix fraction, LBO margin increases, as pilot jets are primarily responsible in the flame stabilization process. As expected, all the new configurations show improved LBO resistance with respect to the baseline case, except for B4, which has straight pilot jets with higher exit velocity (half total outlet area). Looking at the chemiluminescence images of Fig. 3, with standard air B4 layout presents the flame significantly lifted (cases (j) and (k)), especially for the fully diffusive case, and stabilizes at higher distance from the burner outlet with respect to the other configurations. Straight pilot fuel jets intercept the main flow in a region where the premixed jet has high velocity, and the higher fuel jet velocity further lifts off the flame. This does not help in terms of combustion stability, as the flame is subjected to higher strain. As a consequence, flame loss is approached earlier, resulting in the worst LBO margin among the investigated configurations. The leanest condition is instead reached with B1 layout, with outward swirled holes and increased total pilot exit area, therefore reduced jet velocity. This causes part of the pilot fuel to remain entrapped in the outer recirculation zone and react with the dome effusion cooling air, as it can be seen in Figs. 3(d) and 3(e). When the fuel mass flow rate is decreased to approach LBO, jet velocity is further reduced, and the flame stabilizes attached to the dome in the low velocity area of the outer recirculation zone, where reaction is able to sustain also in globally very lean conditions. As a drawback, for this configuration, high temperatures were recorded in stable conditions (TP_{REF}). Figure 5 shows the temperature measured on the dome cold side, with a thermocouple installed near the liner walls, as reported in the schematic. In general, all the configurations show a decreasing trend with higher premix fraction, because the flame closes toward the burner axis, therefore reducing the thermal load at higher radius where the thermocouple is located. B4 configuration with higher jet velocity shows the lowest thermal load

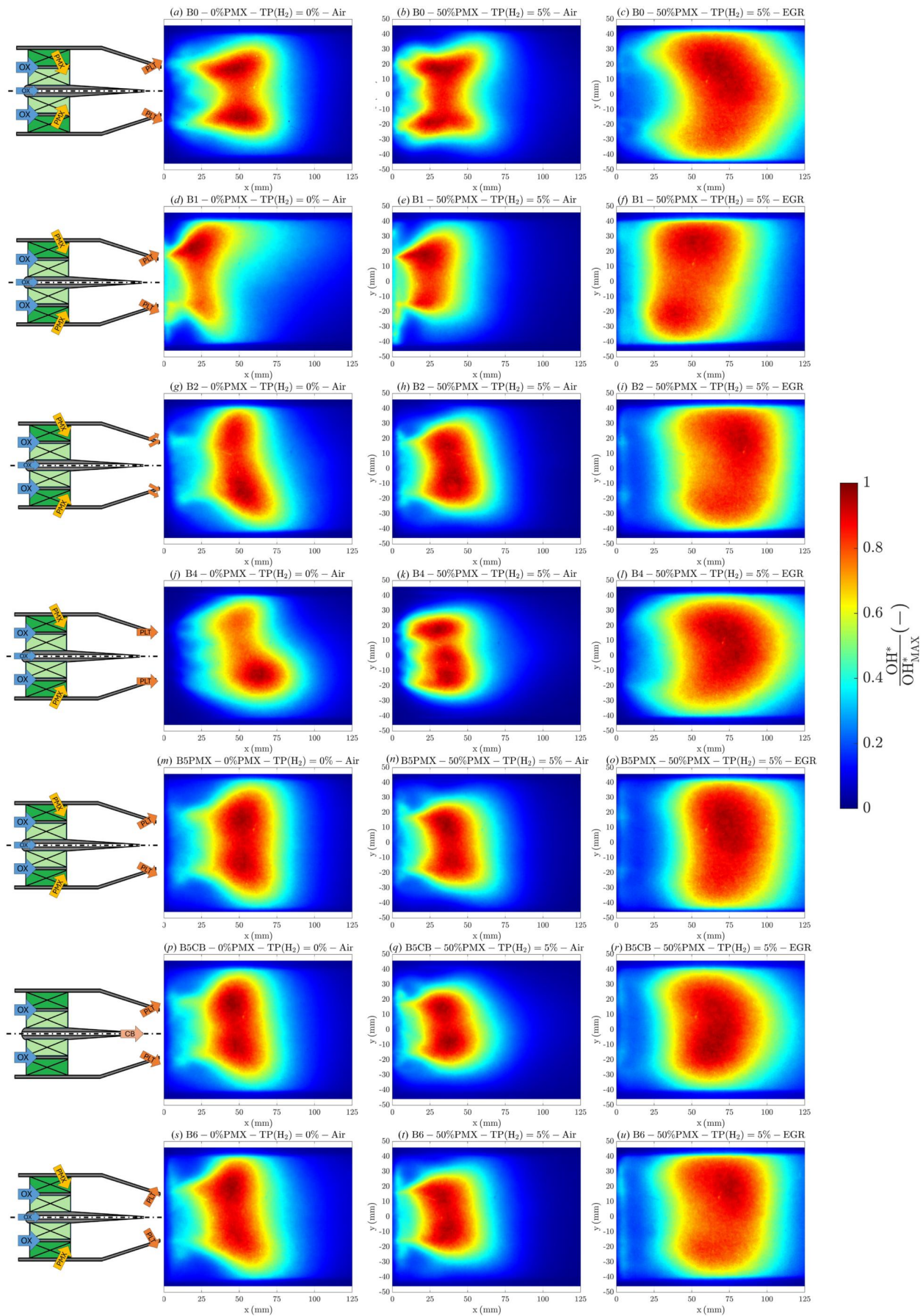


Fig. 3 Normalized OH* chemiluminescence images

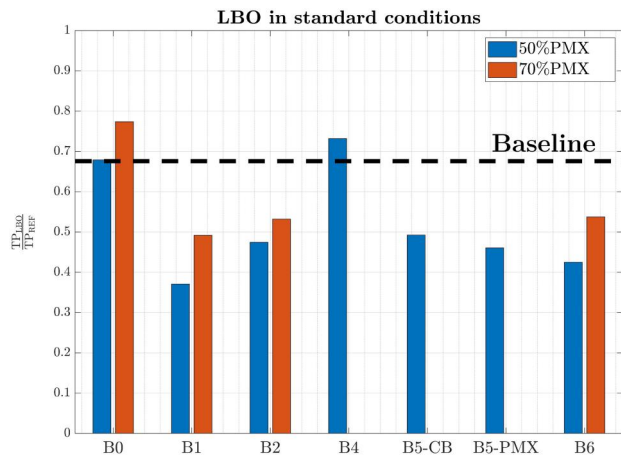


Fig. 4 LBO limits for different burner configurations with 100%NG and standard air as oxidizer

on the dome, as the flame is more lifted, with negative consequences on combustion stability, confirmed by LBO measurements. The highest temperatures are recorded for B1 configuration, particularly when the premix fraction exceeds a certain threshold. In fact, by reducing the pilot fraction and thus the pilot jet velocity, jet penetration is diminished, similarly to what occurs when reducing the fuel flow to approach LBO conditions, and pilot fuel reacts with the dome cooling air. Further increasing the premix does not lead to an increase in the measured temperature, probably because the small differences in the holes exit cause a nonsymmetrical distribution of the reaction zone, as it can be observed in Fig. 3(e), and only a single thermocouple is present. Overall, no damages or alterations were detected, neither on the burner outlet nor on the dome. At engine conditions, such behavior would be emphasized, but managing this effect would require a dedicated design of the cooling system, with possible drawbacks on other design aspects.

For all the new configurations, premix fuel is injected at the tip of the outer swirler (except B5-CB), while for the baseline case injection point is located in the inner swirler. B5 configuration has outwardly oriented pilot jets, similar to the baseline layout. Injecting the premix fuel in the outer swirler promotes the interaction with the pilot flames, giving rise to a more compact reaction zone with respect to the baseline case, as visible in Fig. 3(n). This has positive effects on the LBO margin, as shown by the significant gain in this aspect comparing the baseline case with B5-PMX. The same pilot layout has been tested also injecting the fuel with the center-body along the burner axis, in configuration B5-CB. In this configuration,

premixed fuel is injected along the axis, closer to when it is injected on the internal swirler in terms of position, but lower mixture uniformity is achieved due to shorter premixing length. Also, in this case, the flame results more compact than the baseline case (see Fig. 3(q)), and the lower premixing level promotes locally richer condition which helps in stabilizing the flame. Indeed, the LBO margin is improved with respect to the baseline configuration, slightly lower than B5-PMX as the interaction between premix and pilot fuel is decreased.

Considering only the effect of the pilot holes orientation with premix fuel injected in the outer swirler, LBO margin is slightly improved for B6 with respect to B5-PMX. For B6 layout, with double outward angle of the pilot jets, enhanced interaction between pilot fuel and outer recirculation zone is present, as proved by the smears of OH* intensity at the flame base in this area for 50%PMX and [TP(H₂) = 5%] (Fig. 3(t)). Indeed, improved resistance to blow out is recorded because of the greater recirculation of activated radicals at the flame base, supporting flame stabilization.

The effect of increasing the number of pilot jets was studied with configuration B2, with nominally the same jets exit velocity of the baseline. The double number of jets should reduce the jet penetration and improve the mixing process. LBO resistance is better than the baseline, but it is almost the same as the B5-PMX, which has same premix system. Therefore, the specific effect of the pilot holes number is limited, and the main difference in terms of blow-out margin comes from the enhanced interaction between pilot and premix fuel that is established with the injection of the premix fuel in the outer swirler.

Overall, new configurations with premix fuel injected in the outer swirler generally show improved LBO margins due to enhanced interaction between pilot flames and the premix zone, resulting in more compact reaction zones. The B1 layout with reduced jet velocity achieved the leanest conditions, but this configuration led to other disadvantages in terms of flame position and dome heat load, as highlighted above. B5-PMX and B6 offered significant stability gains through better recirculation at the flame base with outwardly oriented pilot jets, while increasing the holes number (B2) showed limited additional benefit compared to improved premix–pilot interaction.

While the new configurations demonstrated improved lean blow-out resistance compared to the baseline, this comes at the expense of worsened dynamic behavior. Enhanced interactions between pilot and premix fuel reactions, while beneficial for LBO margin, can amplify pressure oscillations and exacerbate thermoacoustic instabilities, potentially limiting overall performance. For the baseline configuration, the outbreak of thermoacoustic instabilities was observed at high premix splits, and Fig. 6 summarizes this aspect for all the investigated burner layouts. Results are reported in terms premix fraction stably achievable. Tests are performed at

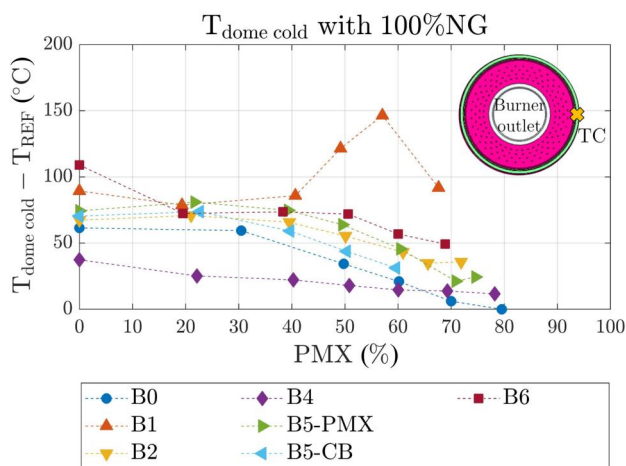


Fig. 5 Temperature measured on the dome cold side for 100%NG and T_{REF}

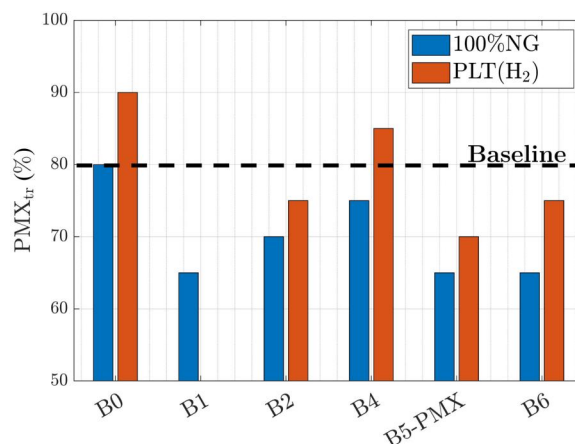


Fig. 6 Premix fraction stably achievable for different burner configurations with standard air as oxidizer

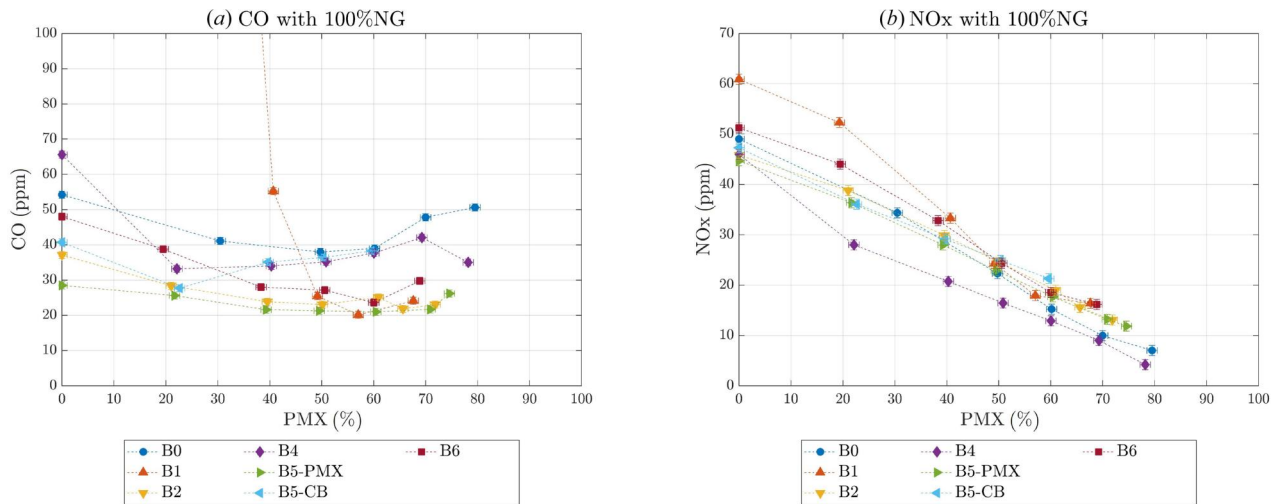


Fig. 7 Pollutant emissions measured with standard air as oxidizer and 100%NG

constant total thermal power, with pure hydrogen injected with the pilot line ($TP_{H_2} = TP_{PLT}$), and gradually increasing the premix fraction until an amplitude threshold of pressure oscillations is reached. For the baseline case with only natural gas, pressure oscillations increase sharply when the premix fraction overcomes 80%PMX, and hydrogen injection allows to shift this limit to 90%, therefore widening the burner operating window [20]. For the B5-CB case, premix fraction has to be kept under 60%PMX because of facility limitations in the fuel upstream pressure, and this aspect could not be investigated. With respect to the baseline case, this aspect is worsened for all the new configurations, with oscillation rising for lower values of the premix fraction. Injecting hydrogen with the pilot line widens the stable region, with slightly different extent depending on the configuration. As the premix system is different for the new burner layouts (B1–B6), these results indicate that injecting the fuel in the outer swirler leads to better resistance to lean blow out due to the increased interaction with the pilots and the external recirculation zone, but at the same time the flame is more sensitive to local equivalence ratio fluctuations at high premix fractions. In general, it is worth noticing that the configurations with worst LBO limits (B0 and B4) show instead the capability to stably reach higher premix fractions, and the effect of hydrogen addition is more beneficial for such configurations. A possible interpretation of this behavior could be linked with the flame lift off. Indeed, detaching the flame base from the burner outlet increases the strain to which the flame is subjected therefore worsening flame stability, but at the same time helps in dampening fluctuations of the local flow, with the lift off height acting as a buffer, with positive effects on the dynamic behavior.

Concluding the burner characterization without EGR, Fig. 7 shows CO and NO_x emissions measured for the different layouts varying the premix thermal power split, with only natural gas.

As expected, NO_x levels decrease linearly with growing premix fraction for all the burner configurations. Diffusive pilot flames are mainly responsible for NO_x production due to local quasi-stoichiometric conditions, which, on the other hand, are crucial in the stabilization process. Comparing the results of B0, B5-PMX, and B5-CB, which have similar pilot holes and different premixing strategies, NO_x levels are almost the same for all the tested fuel split. This means that all these premixing strategies are effective, thanks to the airflow high velocity and strong turbulence created by the swirlers, and differences are limited. B4 layout shows the lowest NO_x levels, further reinforcing the concept that faster and less open pilot jets mix better with the oxidizer. Indeed, by detaching the flame from the nozzle outlet, lifted flames provide a high premixing level in the reaction zone, with beneficial effect on NO_x emissions, especially at low premix fraction. Results of B1 layout, with reduced jet velocity, also confirm this behavior, as NO_x values are higher than the other

configurations, overall indicating poor mixing, confirmed also by very high CO emissions at low premix (not included in the scale of Fig. 7(a) in order to better compare the other configurations). The dependency of CO emission on the premix fraction is reduced, but all the burner configurations exhibit the same nonmonotonic trend. CO levels are substantially lower for the B5-PMX case, because of the higher interaction between outwardly oriented pilot jets and premix fuel injected in the outer swirler. Focusing on the effect of pilot orientation, B6 shows slightly higher values for both CO and NO_x levels with respect to B5-PMX, with decreasing difference as the premix fraction increases. This again could be linked with the mixing process, which is improved as the pilot jets interact more with the oxidizer main flow. Therefore, with more open pilot jets (B6), a lower level of premixing is achieved, but increasing the premix fraction this effect is reduced. Overall, new configurations show lower CO levels, with promising results for the application with EGR, as this aspect is one of the main issues in such conditions.

This performance screening has highlighted how injection of the premix fuel in the outer swirler generally improves CO emissions and lean blow-out resistance, but at the cost of increased dynamic

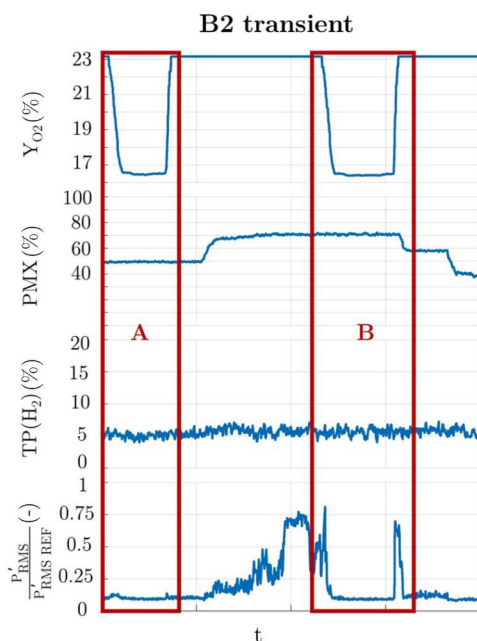


Fig. 8 Transient behavior with simulated EGR for B2

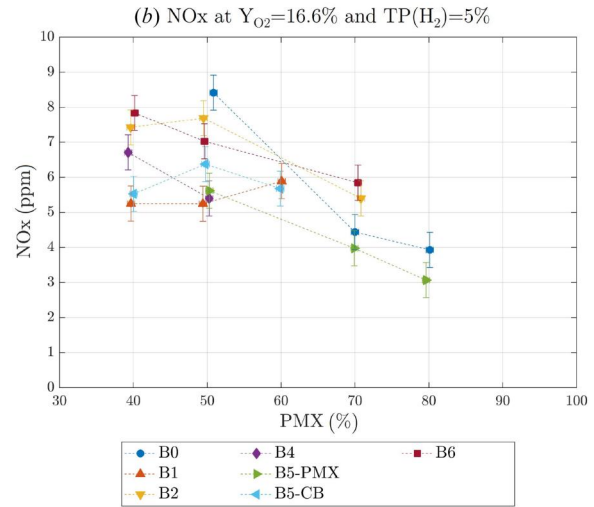
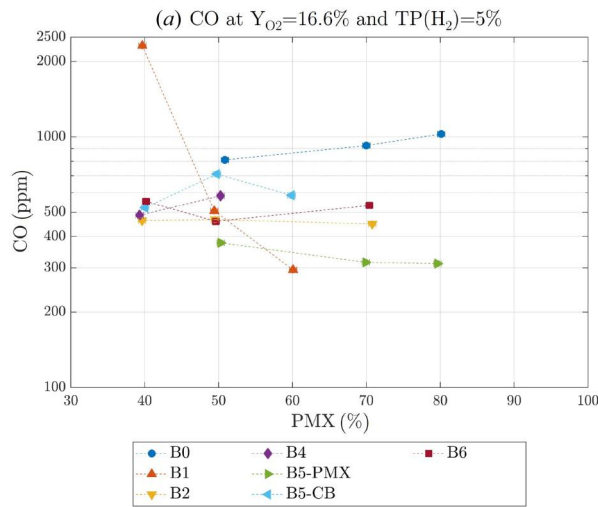


Fig. 9 Pollutant emissions measured with 50%PMX- $Y_{O_2}=16.6\%$ and $TP(H_2)=5\%$

instability, with some differences arising from the varying pilot jet configurations.

Simulated Exhaust Gas Recirculation Conditions. Moving to EGR conditions, the different burner layouts have been compared in terms of NO_x and, more importantly, CO emissions. Indeed, with EGR, NO_x levels are already low as a consequence of the reduced reactivity and the widespread reaction zone, while CO emissions critically rise. Furthermore, for the baseline configuration, thermoacoustic instabilities have been detected when the oxidizer composition varies, with a nonmonotonic dependence on the inlet oxygen content and a positive effect of hydrogen injection. This aspect was investigated also for the new layouts, as showed in Fig. 8, presenting as an example the behavior of B2 configuration. In particular, the amplitude of pressure oscillations inside the combustion chamber is reported (last plot) as the operating conditions vary in terms of inlet oxygen level, premix fraction, and hydrogen content. The red rectangles highlight the conditions with simulated EGR, following the decrease in the oxygen inlet content reported in the first plot.

With simulated EGR, no thermoacoustic instabilities are observed with PMX up to 50% (Fig. 8, point A). However, at higher premix fraction (70% PMX and $TP(H_2)=5\%$, Fig. 8, point B), reducing the inlet oxygen content initially lowers the amplitude of pressure oscillations caused by high premixing. When the oxygen content is further reduced, the amplitude first reaches a peak before dropping significantly, indicating that intermediate conditions are critical at this level of premixing. As the oxygen level increases returning to standard conditions, the oscillations rise again but eventually disappear as the premix fraction decreases. To minimize the exposure of the quartz liner to intense oscillations, the transient was kept rapid, and tests at higher premix levels were not conducted. Similar behaviors have also been observed for other configurations, but they are not reported here for the sake of brevity. In general, higher premix fractions are always more unstable, and the configurations that show more stable behavior without EGR maintain lower oscillation amplitude also with lower oxygen levels.

Regarding emission performance, Fig. 9 reports CO and NO_x values recorded at $Y_{O_2} = 16.6\%$ with constant hydrogen fraction of 5%. It is difficult to identify a general trend with the premix level for CO, while NO_x remains decreasing with higher premix fraction. The beneficial effect of EGR on NO_x emissions overcomes the differences between the different layouts, and all the tested configurations show similar values, which are very low.

High CO emissions are instead one of the main drawbacks of EGR, and indeed represent the major performance parameter for

evaluating the burner capabilities. Contrary to what it was observed for NO_x , the influence of the fuel injection mode on CO emissions is considerable, and some configurations have improved performance. In particular, all the new configurations show lower CO levels than the baseline, except B1 at low premix, which shows high CO values also without EGR at low PMX. The most promising layouts are B5-PMX, B2, and B6, which are able to stay under 500 ppm, which also in standard conditions showed lower CO values (see Fig. 7(a)). All these configurations have outwardly oriented pilot jets and premix fuel injected in the outer swirler. Increasing the number of holes or enhancing the outward orientation of the pilot jets does not improve CO emissions; instead, both changes result in a slight increase. Looking at the steady flame structure (Figs. 3(i), 3(o), and 3(u)) in this condition, differences are negligible and the reaction zone is similar. Some differences are instead visible for B1 configuration, with the lower pilot jet velocity that makes the reaction zone able to stay more attached to the burner also in EGR conditions. The overall length is also reduced with respect to the other configurations (see Fig. 3(f)). As observed in standard conditions, for this configuration also with EGR, CO emissions strongly vary with the premix fraction, with the highest and lowest recorded values. The very high CO levels at low premix are probably linked to the problematic behavior encountered with the fuel reacting with the dome cooling air. However, looking at the results at higher premix levels, a lower jet velocity could help reduce CO emissions and should be investigated more in detail.

The effect of the hydrogen amount has also been evaluated, even though the leeway on this parameter is limited because it is desired to keep the CO_2 content in the exhaust high. Two different levels were tested, equal to 5% and 10% of the total thermal power, keeping the premix fraction constant at 50%PMX, with the results reported in Fig. 10. Increasing the hydrogen fraction has a beneficial effect on CO emissions, which decrease for all the tested configurations. The gain is quite relevant in all cases, and since the effect of reduced carbon content when increasing the hydrogen fraction is negligible, this highlights how higher hydrogen amounts improve CO emissions, while remaining low to limit the reduction of CO_2 in the exhaust. NO_x values are also reported for completeness, which do not show a significant effect of the hydrogen amount. For the baseline configuration, a slight decrease is recorded as hydrogen increases, while for the other configurations values are very similar. It is important to emphasize that all recorded values are single digits, thanks to the beneficial effect of EGR.

Layout B4 was conceived with the purpose to contrast a behavior observed with the baseline configuration, where with pure hydrogen jets at very high premix fraction two separate reaction zone arise, and the premixed natural gas flame front detaches from the hydrogen

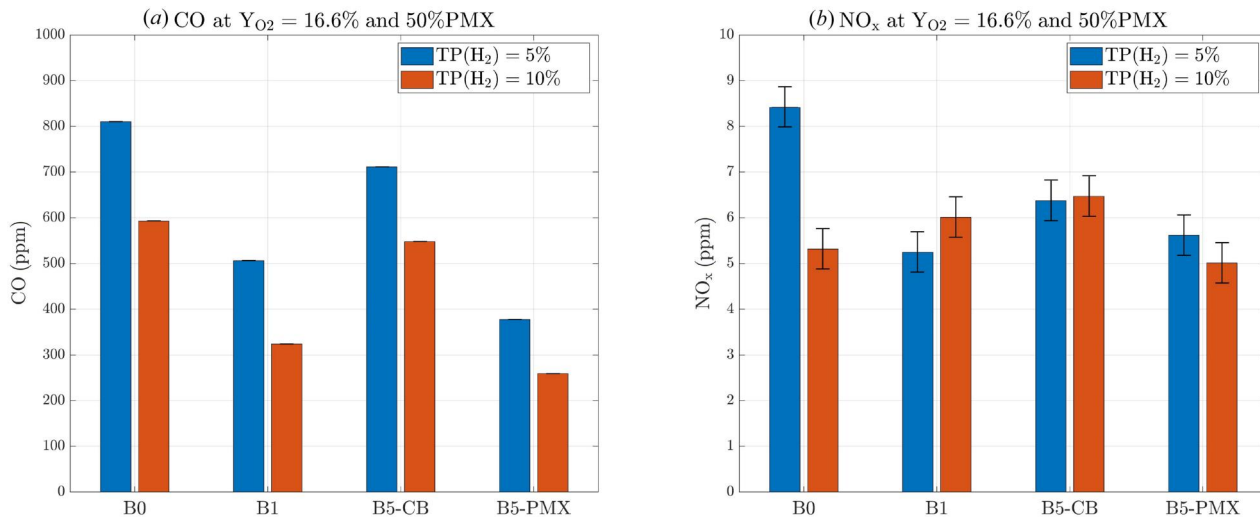


Fig. 10 Pollutant emissions measured with 50%PMX–Y_{O2} = 16.6%

pilots, as shown in Fig. 11. EGR conditions further separate the two reaction zones, with the pilot jets that continue to burn well attached to the burner outlet and the natural gas flame shifting downstream and becoming more widespread. Straight pilot jets with higher velocity adopted in the B4 configuration aimed to enhance the interaction between hydrogen pilots and premixed natural gas in order to reduce CO emissions. OH* images of Fig. 11 show that the two reaction zones remain separated in this condition also for B4 configuration, without a significant improvement on this aspect with respect to the baseline case. Indeed, CO emissions are about the same in this condition, as reported in Fig. 12. Faster hydrogen jets

are not sufficient to increase the interaction between the two separated flame fronts, and this behavior is mainly driven by the high core velocity of the main-flow jet, which causes the premixed natural gas reaction zone to stabilize very far from the burner exit. NO_x values are also reported, with negligible differences between the two configurations. At this very high level of premix, the recorded values are extremely low, even with standard air as oxidizer, and the beneficial effect of EGR is limited. For the baseline configuration, a slight decrease is recorded as hydrogen increases, while for the other configurations values are very similar.

Performance Summary. All the data presented in this work constitute an extensive dataset characterizing the performance of the tested configurations. To provide a final synthesis, the variation of key performance parameters for each configuration was evaluated relative to the baseline case. This study aims to maintain a general approach, focusing on different factors and their correlation with the injection system geometry, and providing valuable insights into flame behavior under both standard and EGR conditions. A single performance indicator could streamline comparison and configuration selection, but defining a comprehensive weighting function for all parameters is challenging due to varying operational contexts and falls out of the scope of this research. Specifically, to summarize the performance of the different burner configurations, the following metrics were analyzed:

- **LBO Air:** LBO margin without EGR at 50%PMX
- **P' NG Air:** Stable premix limit achievable with natural gas and air as oxidizer

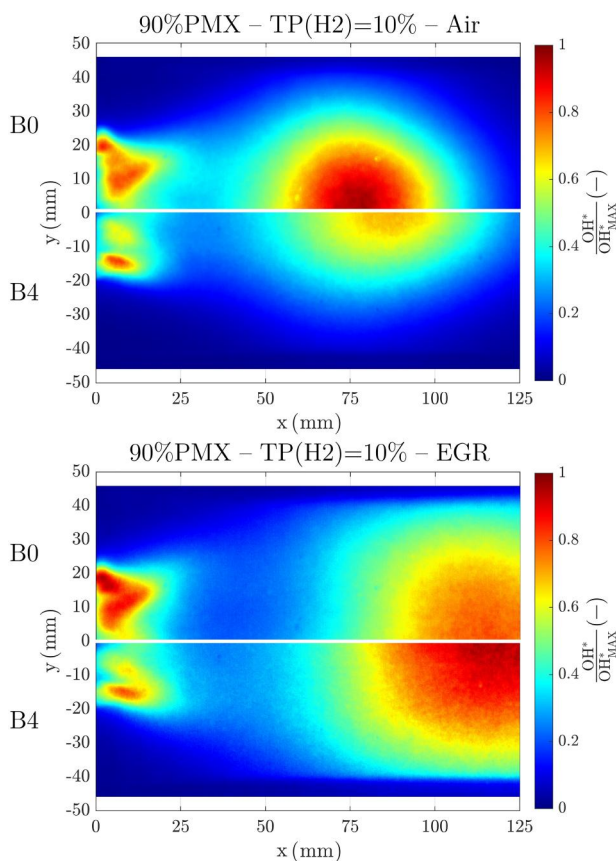


Fig. 11 Normalized OH* chemiluminescence images at 90%PMX and [TP(H₂) = 10%] w/o EGR: comparison of B0 and B4

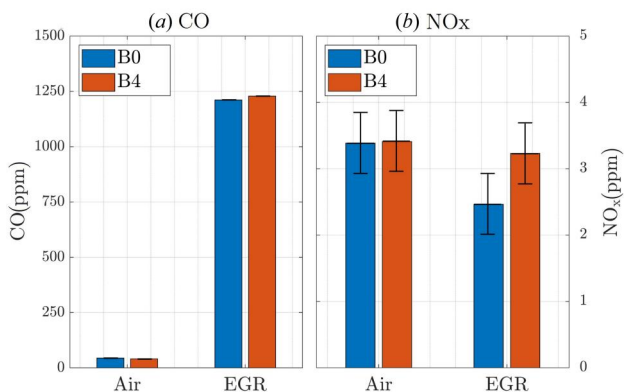


Fig. 12 Pollutant emissions for B0 and B4 at 90%PMX and TP(H₂) = 10%

- **P'' H₂ Air:** Stable premix limit achievable with 100%H₂ pilots and air as oxidizer
- **NO_x Air:** NO_x emissions with natural gas and air as oxidizer
- **CO Air:** CO emissions under standard conditions with natural gas and air as oxidizer
- **NO_x EGR:** NO_x emissions with simulated EGR conditions
- **CO EGR:** CO emissions with simulated EGR conditions

Regarding emissions, values with and without EGR were measured at different fuel splits and averaged for each configuration. The tested split levels are similar across the various configurations, and averaging the values should not significantly affect the results. The dynamic behavior under EGR conditions is challenging to quantify due to the wide variation in operating conditions and thus has not been captured with a single metric. The variation of these parameters with respect to the baseline case has been scaled with the maximum variation of each quantity, to allow a better visualization of the differences, and to be able to present different aspects in a single plot. These parameters were defined based on the specific conditions investigated and the type of analysis performed, and serve primarily to offer a general indication of each configuration's behavior relative to the baseline case. Among the parameters analyzed, CO emissions under EGR conditions can be considered the most critical for the final targets of this research, with LBO limits also holding valuable meaning. NO_x emissions under EGR conditions are of limited importance, as they are already very low in such conditions across all configurations. Conversely, NO_x and CO levels measured with standard air as the oxidizer hold greater relevance for burner operation in conventional applications.

Figure 13 summarizes the results for all the new layouts, allowing to identify the most critical and the most promising aspects for each configuration, and providing valuable insight into where optimization efforts might be most effective. As noted earlier, it is observed that configurations with better lean blowout margins tend to exhibit worse dynamic stability.

Overall, some configurations demonstrate promising results, outperforming others. Among these, B5-PMX layout appears to be the most effective solution investigated, featuring premix fuel injected into the outer swirler and axisymmetric pilot jets oriented outward at the same angle as the baseline. The B2 configuration also

shows potential, with an improved pilot fuel distribution due to the increased number of holes. However, both configurations exhibit significantly worse dynamic stability limits compared to the baseline, an issue that will need to be addressed in future developments.

Conclusions

The present study explored the performance of different configurations of a dry low NO_x industrial burner under both standard conditions and simulated EGR. Tests were performed at atmospheric pressure with natural gas, eventually doped with hydrogen on the pilot line to mitigate the challenges posed by reduced oxygen levels. A total of seven burner configurations including the baseline were tested, varying the fuel injection strategies for both pilot jets and premixing system, to evaluate their impact on key performance metrics such as emissions, stability limits, and dynamic behavior. The significant variation in operating conditions due to the unconventional application of EGR in gas turbines and the dual-fuel configuration, combined with the challenges of testing real hardware components, makes the burner behavior extremely complex.

The results highlight the critical role of the external recirculation zone in influencing flame behavior, particularly in the absence of an inner recirculation zone due to low swirl from the counter-rotating swirler configuration. When fuel is retained in this zone thanks to higher external orientation of the pilot jets or lower jet velocity, blowout resistance improves, but the flame also becomes more susceptible to thermoacoustic instabilities. Decreasing the pilot jet velocity brings benefits for the LBO margin but for the investigated configuration problems were found in normal operation. Moving the premix fuel injection point in the outer swirler also positively affects CO emissions and lean blow-out margin because of the enhanced interaction between premix and pilot fuel, again at the cost of lower dynamic stability. In EGR conditions, high CO emissions are the main limiting factor, and positive results have been encountered for the new configurations with respect to the baseline, with a significant reduction of measured CO levels. The dynamic behavior is also conditioned by EGR, representing another aspect to be addressed during the design and optimization processes in order to ensure the reliability, efficiency, and stability in real gas turbine applications.

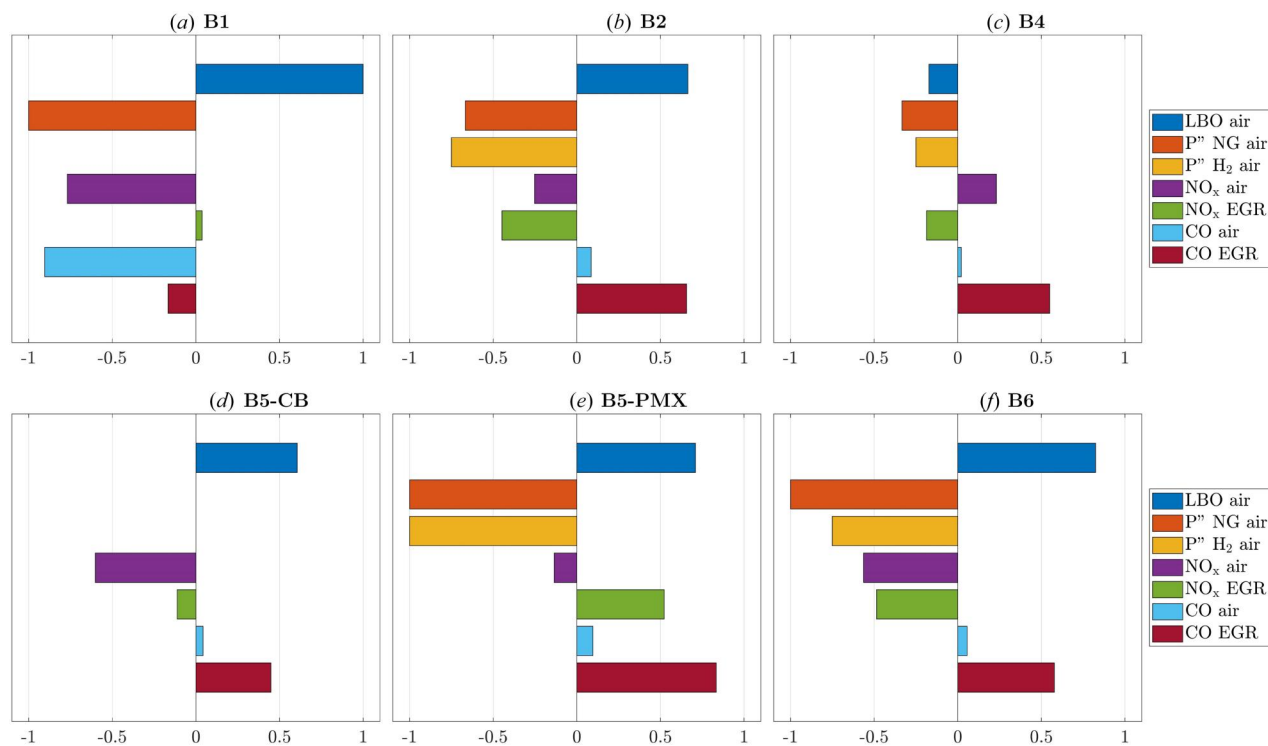


Fig. 13 Performance summary for each burner configuration

In conclusion, the present study remarks the importance of dedicated experimental investigations to understand the flame behavior and stabilization mechanisms, with the final purpose of enhancing the performance of modern combustion systems under unconventional and demanding operating conditions. The collected results allowed for an understanding of the influence of control parameters and how they can be leveraged, highlighting the positive effects of hydrogen addition and the impact of fuel injection methods. In addition, the extensive data gathered during this work could be valuable for validating numerical models, particularly when analyzing unstable phenomena such as lean blowout or nonconventional conditions involving oxidant mixtures with reduced oxygen levels. Indeed, the combustion regimes resulting from the dual fuel operation into an oxygen depleted environment are particularly challenging to predict, and numerical models can greatly benefit from dedicated experimental investigations with optical diagnostics.

Within the Transition project framework, a restricted number of the presented burner configurations will be subjected to testing at high pressure, along with new designs optimized through numerical analysis utilizing the data gathered in this study. This next phase of the project involves an increase in the complexity of the experimental setup, aiming to a more accurate representation of the conditions experienced in real combustion systems, further contributing to the development of more efficient and reliable combustion technologies able to operate with high EGR rates.

Funding Data

- European Union's Horizon Europe Research and Innovation program (Grant Agreement No. 101069665).

Data Availability Statement

The authors attest that all data for this study are included in the paper.

Nomenclature

BH	= Baker Hughes
CB	= center-body fuel line
CCS	= carbon capture and storage
D	= pilot holes diameter (mm)
EGR	= exhaust gas recirculation
f_{aq}	= acquisition frequency (Hz)
FoV	= field of view
GT	= gas turbine
LBO	= lean blow out
N	= pilot holes number
NG	= natural gas
OX	= oxidizer
P_{RMS}^p	= root mean square of pressure oscillation (mbar)
PLT	= pilot fuel line
PMX	= premix fuel line
PMX%	= premix fuel thermal power fraction (%)
T_{flame}	= adiabatic flame temperature (°C)
T_{inlet}	= inlet temperature (°C)
TP _{REF}	= reference thermal power (kW)
TP _{TOT}	= total thermal power (kW)
TP(H ₂) %	= hydrogen thermal power fraction (%)
x	= axial coordinate (mm)
y	= radial coordinate (mm)
Y_{O_2}	= inlet oxygen mass fraction (%mass)
$\Delta P/P$	= combustor pressure drop (%)
λ	= wavelength (nm)
ϕ	= pilot orientation angle (deg)

References

- [1] Zheng, M., Reader, G. T., and Hawley, J., 2004, "Diesel Engine Exhaust Gas Recirculation—A Review on Advanced and Novel Concepts," *Energy Convers. Manage.*, **45**(6), pp. 883–900.
- [2] Li, H., Ditaranto, M., and Berstad, D., 2011, "Technologies for Increasing CO₂ Concentration in Exhaust Gas From Natural Gas-Fired Power Production With Post-Combustion, Amine-Based CO₂ Capture," *Energy*, **36**(2), pp. 1124–1133.
- [3] Vantaggiato, E., Riboldi, L., Anantharaman, R., Carcasci, C., Andreini, A., Roussanaly, S., and Ditaranto, M., 2024, "Understanding the Potential and the Challenges of a NGCC Integrated With Hydrogen-Assisted EGR and CO₂ Capture," *ASME Paper No. GT2024-125639*.
- [4] Burnes, D., Saxena, P., and Dunn, P., 2020, "Study of Using Exhaust Gas Recirculation on a Gas Turbine for Carbon Capture," *ASME Paper No. GT2020-16080*.
- [5] Elkady, A. M., Evulet, A., Brand, A., Peter Ursin, T., and Lynghjem, A., 2008, "Exhaust Gas Recirculation in DLN F-Class Gas Turbines for Post-Combustion CO₂ Capture," *ASME Paper No. GT2008-51152*.
- [6] Li, H., Elkady, A., and Evulet, A., 2009, "Effect of Exhaust Gas Recirculation on NO_x Formation in Premixed Combustion System," *AIAA Paper No. 2009-226*.
- [7] Røkke, P., and Hustad, J., 2005, "Exhaust Gas Recirculation in Gas Turbines for Reduction of CO₂ Emissions; Combustion Testing With Focus on Stability and Emissions," *Int. J. Thermodyn.*, **8**(4), pp. 167–173.
- [8] Burdet, A., Lachaux, T., de la Cruz Garcia, M., and Winkler, D., 2010, "Combustion Under Flue Gas Recirculation Conditions in a Gas Turbine Lean Premix Burner," *ASME Paper No. GT2010-23396*.
- [9] Guethe, F., Stankovic, D., Genin, F., Syed, K., and Winkler, D., 2011, "Flue Gas Recirculation of the Alstom Sequential Gas Turbine Combustor Tested at High Pressure," *ASME Paper No. GT2011-45379*.
- [10] Evulet, A. T., Elkady, A. M., Branda, A. R., and Chinn, D., 2009, "On the Performance and Operability of GE's Dry Low NO_x Combustors Utilizing Exhaust Gas Recirculation for Post-Combustion Carbon Capture," *Energy Procedia*, **1**(1), pp. 3809–3816.
- [11] Kitagawa, K., Konishi, N., Arai, N., and Gupta, A. K., 2003, "Temporally Resolved Two-Dimensional Spectroscopic Study on the Effect of Highly Preheated and Low Oxygen Concentration Air on Combustion," *ASME J. Eng. Gas Turbines Power*, **125**(1), pp. 326–331.
- [12] Kobayashi, H., Hagiwara, H., Kaneko, H., and Ogami, Y., 2007, "Effects of CO₂ Dilution on Turbulent Premixed Flames at High Pressure and High Temperature," *Proc. Combust. Inst.*, **31**(1), pp. 1451–1458.
- [13] Rodriguez Camacho, J., Akiki, M., Blust, J., and O'Connor, J., 2024, "Effect of Inert Species on the Static and Dynamic Stability of a Piloted, Swirl-Stabilized Flame," *ASME J. Eng. Gas Turbines Power*, **146**(6), p. 061021.
- [14] Oztarlik, G., Selle, L., Poinso, T., and Schuller, T., 2020, "Suppression of Instabilities of Swirled Premixed Flames With Minimal Secondary Hydrogen Injection," *Combust. Flame*, **214**, pp. 266–276.
- [15] Barbosa, S., de La Cruz Garcia, M., Ducruix, S., Labegorre, B., and Lacas, F., 2007, "Control of Combustion Instabilities by Local Injection of Hydrogen," *Proc. Combust. Inst.*, **31**(2), pp. 3207–3214.
- [16] Shanbhogue, S. J., Sanusi, Y. S., Taamallah, S., Habib, M. A., Mokheimer, E. M. A., and Ghoniem, A. F., 2016, "Flame Macrostructures, Combustion Instability and Extinction Strain Scaling in Swirl-Stabilized Premixed CH₄/H₂ Combustion," *Combust. Flame*, **163**, pp. 494–507.
- [17] Cheng, R., Littlejohn, D., Strakey, P., and Sidwell, T., 2009, "Laboratory Investigations of a Low-Swirl Injector With H₂ and CH₄ at Gas Turbine Conditions," *Proc. Combust. Inst.*, **32**(2), pp. 3001–3009.
- [18] Du, Y., Yu, X., Liu, L., Li, R., Zuo, X., and Sun, Y., 2017, "Effect of Addition of Hydrogen and Exhaust Gas Recirculation on Characteristics of Hydrogen Gasoline Engine," *Int. J. Hydrogen Energy*, **42**(12), pp. 8288–8298.
- [19] Rodriguez Camacho, J., Le, D., Blust, J., and O'Connor, J., 2024, "Impact of Diluents on Flame Stability With Blends of Natural Gas and Hydrogen," *ASME J. Eng. Gas Turbines Power*, **147**(1), p. 011017.
- [20] Galeotti, S., Picchi, A., Becchi, R., Lemmi, G., Meloni, R., Babazzi, G., Giannini, N., Facchini, B., and Andreini, A., 2024, "Experimental Study on Stability Enhancement of a Natural Gas GT Burner With Hydrogen Flame Piloting Operated With Simulated Exhaust Gas Recirculation," *ASME Paper No. GT2024-128732*.
- [21] Galeotti, S., Picchi, A., Becchi, R., Meloni, R., Babazzi, G., Romano, C., and Andreini, A., 2024, "Experimental Characterization of an Industrial Burner Operated With Simulated EGR," *Appl. Therm. Eng.*, **246**, p. 122943.
- [22] Babazzi, G., Galeotti, S., Picchi, A., Becchi, R., Cerutti, M., and Andreini, A., 2024, "Combustion Diagnostics and Emissions Measurements of a Novel Low NO_x Burner for Industrial Gas Turbine Operated With CO₂ Diluted Methane/Air Mixtures," *ASME J. Eng. Gas Turbines Power*, **146**(7), p. 071007.
- [23] Joshi, N. D., Epstein, M. J., Durlak, S., Marakovits, S., and Sabla, P. E., 1994, "Development of a Fuel Air Premixer for Aero-Derivative Dry Low Emissions Combustors," *ASME Paper No. 94-GT-253*.
- [24] Innocenti, A., Andreini, A., Facchini, B., Cerutti, M., Ceccherini, G., and Riccio, G., 2016, "Design Improvement Survey for NO_x Emissions Reduction of a Heavy-Duty Gas Turbine Partially Premixed Fuel Nozzle Operating With Natural Gas: Numerical Assessment," *ASME J. Eng. Gas Turbines Power*, **138**(1), p. 011501.
- [25] Andreini, A., Facchini, B., Innocenti, A., and Cerutti, M., 2014, "Numerical Analysis of a Low NO_x Partially Premixed Burner for Industrial Gas Turbine Applications," *Energy Procedia*, **45**, pp. 1382–1391.